# Structure and spectra of a confined HeH molecule

**J M H Lo[1], M Klobukowski[1], D Bielińska-Wąż[2], E W S Schreiner[3] and G H F Diercksen[3]**

[1] Department of Chemistry, University of Alberta, Edmonton, Alberta, Canada T6G 2G2

[2] Instytut Fizyki, Uniwersytet Mikołaja Kopernika, ul. Grudziądzka 5, 87-100 Toruń, Poland

[3] Max-Planck-Institut für Astrophysik, Karl-Schwarzschild-Straße 1, D-85741 Garching, Germany

E-mail: `mariusz.klobukowski@ualberta.ca`

**Abstract.** The influence of spatial confinement on the structure and spectra of the Rydberg HeH molecule is analyzed at the level of the variational full configuration interaction approach. The confining potential is assumed to have cylindrical symmetry, with the symmetry axis of the potential overlapping with the molecular bond. In the direction perpendicular to the axis quadratic dependence of the potential on the electron coordinates is assumed. The influence of the confining potential on the form of the potential energy curves (in particular on the bond lengths), on the electronic spectra, and on the ionization due to the confinement is studied in detail.

PACS numbers: 31.15.Ar, 31.25.Nj, 31.90.+s, 78.67.De

Submitted to: *J. Phys. B: At. Mol. Opt. Phys.*

## 1. Introduction

The effects of environment on the properties of atoms and molecules (e.g. the influence of plasmas [1, 2], external magnetic fields [3], and surfaces [4, 5]) are frequently modeled as confining potentials. Reviews of the subject were written by Jaskólski [6] and, more recently, by Connerade [7, 8]. The influence of confining potentials on properties of atoms has been analyzed extensively by several authors [9, 10, 11] and a few studies on confined molecules have also been published. One should mention a detailed study of the $H_2$ molecule confined by a spherical harmonic potential [12] and another on $H_3^+$ and $H_2$ in cylindrical confinement [13]. A detailed analysis of the $Li_2$ confined by anisotropic harmonic potentials was published [14] and the effects of a cylindrical confining potential on the excited states of the $H_2$ molecule were studied [15]. In the work on the $H_2$ molecule [15] the cylindrical harmonic confining potential was related to the magnetic field parallel to the molecular axis.

In the present work we report and analyze the effects of confinement on the structure and spectra of the HeH molecule. The helium hydride molecule is one of the smallest diatomic molecules and it has been a subject of theoretical studies for over forty years. Early molecular orbital studies predicted that HeH should possess a repulsive ground state but bound excited states [16]. Subsequent multi-reference configuration interaction calculations by Theodorakopoulos et al. also yielded the same conclusion [17]. However, no experimental evidence was available for the existence of bound excited electronic states of HeH until the detection of the $B^2\Pi \rightarrow X^2\Sigma^+$ fluorescence of HeH via the reactive collision of excited $H_2$ and He [18] in 1985. Following this observation, several studies were devoted to the measurement and analysis of the bound-free radiative decay and predissociation of these states [19, 20, 21, 22]. Up to now, about 14 states, corresponding to $n \leq 4$, have been fully characterized [23, 24, 25, 26] and many high-lying states ($11 \leq n \leq 34$) have been detected by employing the field ionization technique [27]. In addition, a series of bound states (for $n = 5$) was located by the scattering R-matrix method [28].

Despite its simplicity, the HeH molecule exhibits unique properties in powerful UV lasers [29]. Noble gas hydrides belong to the family of Rydberg (or excimer) molecules characterized by their unstable electronic ground state and bound excited states [30]. The stability of the excited states of HeH has been ascribed to the polarization of He by the $H^+$ core when the H(1s) electron is excited. The resulting system can thus be regarded as a pair formed by the $HeH^+$ ion and an electron. The Coulombic interaction between the pair is rather weak and the Rydberg electron is sensitive to any kind of external perturbation. Therefore, the effects of spatial confinement should be evident even when a relatively weak perturbation is applied.

Two particular effects were investigated in the present work. The first effect is the influence of the confining potential on the shape of the potential energy curves, i.e., the vibronic spectra. To obtain a better understanding of this effect, the ground and the first few excited singlet states of HeH were calculated for several values of the potential strength and a wavefunction analysis in terms of the orbital response to the external potential was performed. The second effect is the ionization process induced by confinement. The values of the parameters defining the strength of the confinement under which the molecule in a given electronic state becomes ionized due to the confinement were determined.

## 2. Theory

The Hamiltonian of a confined $N$-electron diatomic molecule is taken as

$$\hat{H}_\omega(\boldsymbol{r}, R) = \hat{H}_0(\boldsymbol{r}, R) + \mathcal{W}_\omega(\boldsymbol{r}), \tag{1}$$

where

$$\hat{H}_0(\boldsymbol{r}, R) = \hat{T}(\boldsymbol{r}) + \hat{V}_{en}(\boldsymbol{r}, R) + \hat{G}(\boldsymbol{r}) + \hat{V}_{nn}(R), \tag{2}$$

is the Born-Oppenheimer Hamiltonian of the free system, $\hat{T}(\boldsymbol{r})$, $\hat{V}_{en}(\boldsymbol{r}, R)$, $\hat{G}(\boldsymbol{r})$, and $\hat{V}_{nn}(R)$ represent, respectively, the operators describing the kinetic energy, the nuclear attraction potential, the electron and nuclear repulsion potentials; $\boldsymbol{r} \equiv \{\boldsymbol{r}_1, \boldsymbol{r}_2, \ldots, \boldsymbol{r}_N\}$ stands for the electron coordinates and $R$ denotes the internuclear distance. The $N$-electron confining potential $\mathcal{W}_\omega(\boldsymbol{r})$ is defined as a sum of one-electron contributions

$$\mathcal{W}_\omega(\boldsymbol{r}) = \sum_{i=1}^{N} W_\omega(\boldsymbol{r}_i), \tag{3}$$

where $\boldsymbol{r}_i = \{x_i, y_i, z_i\}$. In the present work it is assumed that the molecular axis overlaps with the z-axis of the coordinate system and that the confining potential is of the form of the cylindrical oscillator potential

$$W_\omega(\boldsymbol{r}_i) = \frac{\omega^2}{2}(x_i^2 + y_i^2). \tag{4}$$

As the strength of the confinement increases, the total energy of the electronic states of a confined HeH molecule containing three electrons increases faster than the total energy of the two-electron positive ion $HeH^+$ in its electronic ground state. Therefore there exists a critical confinement parameter $\omega_c$ for each electronic state. For the values $\omega > \omega_c$, the energy of the neutral molecule exceeds that of the ion. For confinements stronger than the critical confinement the corresponding electron is bound by the confining potential rather than by the nuclei and its energy spectrum is mainly determined by the form of the confinement. This behaviour is related to the *autoionization of atoms by pressure* [7, 31].

## 3. Computational method and basis sets

The full configuration interaction (FCI) method, as implemented in the programs OpenMol [32] and GAMESS-US [33, 34], was used to find the solutions of the electronic Schrödinger equation for the $n$-th electronic state of HeH

$$\hat{H}_\omega(\boldsymbol{r}, R)\Psi_\omega^n(\boldsymbol{r}, R) = E_\omega^n \Psi_\omega^n(\boldsymbol{r}, R), \tag{5}$$

where the state index $n$ equals $0, 1, 2, 3, 4, 5$, and 6 for the states $X\,^2\Sigma^+$, $A\,^2\Sigma^+$, $B\,^2\Pi^+$, $C\,^2\Sigma^+$, $D\,^2\Sigma^+$, $E\,^2\Pi^+$, and $F\,^2\Sigma^+$, respectively. The molecular orbitals for the FCI calculations were obtained by a Hartree-Fock calculation for the lowest $^2\Sigma$ state. The potential energy curves $E_\omega^n(R)$ of the HeH molecule as well as the ground-state potential energy curve $E_\omega^0(R)$ of $HeH^+$ were calculated for several values of the confinement parameter $\omega$.

Four different combinations of He and H basis sets, *vis.* He-21/H-18, He-21/H-36, He-21/H-55, and He-34/H-55, have been tested in order to determine a suitable basis set for the studies of the confined HeH molecule. Two basis sets were used for helium, He-21 and He-34. The first set is derived from Römelt's $7s2p1d$ basis set [35], contracted to $5s2p1d$, and augmented by a set of $2s1p$ diffuse functions ($\alpha = 0.08$ and 0.02 for $s$ and 0.08 for $p$), while the second set is constructed from the He-21 basis set augmented

with $1p2d$ polarization functions [36]. In order to describe the Rydberg character of the first several low-lying excited states of HeH three basis sets of hydrogen, H-18, H-36 and H-55, with different size of the polarization and diffuse spaces have been utilized [36]. The smallest set, H-18, is Huzinaga's $(6s)/[4s]$ basis set [37] augmented by the $2s4p$ diffuse set whose exponents are optimized for the proper description of the long-range interaction of the excited states of $H_2$ [35]. Both the H-36 and H-55 share the same $(13s7p)$ set grouped into a (3,2,1,1,1,1,1,1,1,1/1,1,1,1,1,1,1) contraction. The former possesses an extra $d$-function, leading to a $10s7p1d$ basis set, while in the latter a group of $1s1p4d$ diffuse functions is added, giving rise to a $11s8p4d$ basis set.

The calculated spectroscopic constants for the first six excited electronic states of HeH are shown in table 1. In general, a very good agreement with the available experimental and theoretical data was achieved. The estimated $r_e$ values deviate from the best values by at most 0.01 Å, while the calculated $\nu_e$ agree with the experimental values with an average discrepancy of about 3%.

Despite the overall good performance of these four combinations of basis sets, several differences between the basis sets have been observed. A fairly big discrepancy was seen for both the $r_e$ and $\nu_e$ values of the F $^2\Sigma^+$ state obtained by using the He-21/H-18 basis sets. This is not unexpected since the H-18 basis set lacks $d$-type functions which are essential for accurately describing the $3d$ character of the F state. Inclusion of an additional $d$-type functions and extra $s$- and $p$-type diffuse functions (basis H-36) changed the equilibrium bond lengths and harmonic frequencies for the A to E states only slightly but it greatly improved the $r_e$ value for the F state. Further expansion of the $d$-space (basis H-55) led to the elongation of the equilibrium internuclear distance and to a significant variation of $\nu_e$ for all states. The effects of increasing the diffuse space of the He basis set have also been investigated (basis He-34). The resulting $\nu_e$ values remained approximately unaffected but the $r_e$ values decreased by about 0.003 Å.

Since the low-lying excited states of HeH arise from the excitation of the H $1s$ electron, the estimated excitation energies of the H atom using the H-18, H-36 and H-55 basis sets can serve as an excellent indication of their quality in the molecular studies of the Rydberg HeH molecule. Schreiner has performed a series of atomic calculations on hydrogen with these basis sets and the results revealed that the H-36 basis set is among the best basis sets which yielded excitation energies up to $n = 4$, except for $3d$-orbitals, with an average error of 6 $\mu$Hartree [36].

In consequence, the H-36 basis set was utilized in the subsequent full CI calculations of the low-lying electronic states of HeH in the presence of a harmonic confining potential. In order to enhance the flexibility of the basis set combination He-21/H-36 in the description of the electron density distorted in the presence of confinement an additional set of $1s1p1d$ Gaussian-type functions was added in the middle of the He-H bond. The exponents of these functions were equal to $\omega/2$. The use of such auxiliary basis functions has been justified in the calculations of a confined two-electron system [9], helium atom [11], and lithium molecule [14]. In the present study, the potential energy curves of the ground and low-lying excited states of the HeH molecule were calculated for

confinement parameters ranging from 0.0 to 0.4 au. However, the discussion is focused only on small values of $\omega$ (i.e., $\omega < 0.20$ au) due to the field-induced ionization which will be discussed in the following section.

## 4. Results and Discussion

### *4.1. Potential energy curves of HeH*

Figure 1 shows the potential energy curves of the ground and several low-lying excited states of HeH. In the same figure the ground state potential energy curve of $HeH^+$ is also included for comparison. As may be seen, except for the ground state which exhibits a shallow van der Waals minimum at the internuclear distance of about 7.00 au, the excited states of HeH are all characterized by a deep potential well which is similar to the ground state potential of the molecular ion. An exception is the C $^2\Sigma^+$ state potential where a barrier of 0.6 eV (0.022 au) above the dissociation limit at $R$ of about 4.00 au is present due to the interaction between the Rydberg electron and the He core electrons [17]. It has been predicted that the F $^2\Sigma^+$ state potential energy curve of NeH also contains an energy barrier at 4.5 au [17] which is smaller than the one for the C state. However, an analogous feature is absent in HeH which could indicate a weaker interaction between the core and Rydberg electrons.

The excited states of HeH studied in the present work can essentially be described by a single-reference configuration resulting from the excitation of the hydrogen's $1s$ electron to the Rydberg orbitals. Unlike in the case of NeH, where a strong configuration mixing is observed between the $^2\Sigma^+$ states, Petsalakis et al. found that the non-adiabatic coupling matrix elements between the A and C states are rather small [42]. The A state is dominated by the He + H($2s$) configuration while the C state acquires mainly the H($2p$) character for the whole range of $R$, and they both lead to the same dissociation limit of He + H($2s2p$).

The B state, which is dominated by H($2p$) character, is also correlated to the dissociation products of He and excited H($n = 2$) atoms. This state lies very close to the A state potential energy curve yet it is fairly well separated from that of the C state. This behavior can be attributed to the fact that the $\pi$ molecular orbitals resulting from the hydrogen $2p_x$ and $2p_y$ atomic orbitals are less destabilized by the Coulomb interaction with the He core electron density as compared to the $\sigma$ orbital which is formed from the hydrogen $2p_z$ atomic orbital. As a result, the latter state potential energy curve is shifted towards higher energies for small and intermediate values of $R$. As $R \to \infty$, these two states gradually become degenerate, leading to the same asymptotic limit of He + H($n = 2$).

The potential energy curves of the X to F states of HeH have been computed for several values of the confinement parameter $\omega$ between 0.00 and 0.15 au in order to investigate the effects of the harmonic confining potential on both the spectroscopic and electronic properties of the HeH molecule. The potential energy curves for the six states

were compared with the potential curves of the ground state of $HeH^+$, calculated for the same value of $\omega$. In the following analysis, only those excited states will be discussed whose energies are below that of the $HeH^+$ ion, as the one-particle basis set employed in the present work was not designed for the description of ionization by pressure.

Figure 2 shows the potential energy curves for the A, B and C $^2\Sigma^+$states of HeH together with the ground-state potential energy curves of the ion $HeH^+$ for the same range of $\omega$. As shown, these states behave in substantially different ways under the influence of an external potential. The potential energy curves of both the B state of HeH and the ground state of $HeH^+$ retain the same shape for $\omega \leq 0.15$ au. These states are only shifted to higher energies by the confining potential and become slightly more bound. These observations can be accounted for by the fact that the harmonic potential which increases the electron density between the nuclei through the Coulomb interaction does not significantly enhance the $\pi$-type bonding in HeH. Instead, the Rydberg H($2p$) orbital will become distorted so that the B state is destabilized.

On the other hand, the $^2\Sigma^+$ state potential energy curves of HeH are strongly affected by the confining potential. The characteristic local barrier of the C state potential remains for $\omega > 0.00$ au but its height increases with $\omega$. For instance, the local maximum lies about 0.58 eV (0.021 au) above the limit of He + H($2p$) for $\omega = 0.00$ au. This barrier increases for $\omega = 0.10$ au to 1.07 eV (0.039 au). Simultaneously, the binding energy with respect to the dissociation products increases from 1.01 eV to 1.12 eV (0.037 au to 0.041 au) because of the greater $\sigma$-bonding electron density.

Two interesting and unexpected features occur on the A state potential energy curve due to the confining potential. The first feature is the presence of a potential barrier at 3.00 au when HeH is confined by a cylindrical harmonic potential. A similar situation has also been observed for the NeH molecule [43]. The emerging potential maximum is possibly the consequence of an avoided crossing between the A and C $^2\Sigma^+$ states at the point where they interchange their configurations. The development of the two states with increasing strength of the confining potential is shown in figure 3. At small $R$ the A state still possesses mainly the hydrogen $2s$ character as the free-field counterpart. However, the dominant configuration of the state in the long range region turns out to be He + H($2p_z$). Previous studies have demonstrated that the orbital degeneracy of a hydrogen atom embedded in a prolate-type potential will be partially removed, with the $p_z$ component being more stabilized with respect to $s$ and other $p$-components [9]. Accordingly, when a cylindrical confining potential is applied to HeH, the dissociation channel of He + H($n = 2$) splits, giving rise to three sub-channels. The avoided crossing can thus allow the A and C states to exchange configurations and dissociate to the proper limits. The avoided crossing is less marked in the case of the HeH than in the NeH molecule [43].

The second feature of the A state potential energy curve is the reduction of the binding energy with increasing $\omega$. The binding energy in the case of $\omega = 0.15$ au is 1.70 eV (0.062 au) while in the unconfined case it is equal to 2.53 eV (0.093 au). This change can be rationalized in terms of the avoided crossing. The larger shift of the

H($2s$) potential as compared to that of H($2p_z$) potential causes a decrease of the energy gap between these two states and thus of the binding energy of the A state potential energy curve.

In spite of the complicated changes of the shape of the potential energy curves of different states of HeH the variation of $r_e$, the equilibrium bond distance, is rather small as shown in table 3 and illustrated in figure 4. For $\omega \leq 0.10$ au the average deviation of $r_e$ for these states is less than 3%. This behavior is different from that of a confined $H_2$ molecule where the confinement led to a considerable reduction of the bond length [44].

The values of electric dipole moment were calculated for all states at $R = 1.5$ au and the results are shown in figure 5. Variation of the dipole moments is rather small for the three lowest states and larger for the three highest states. In the latter states the electron density associated with the Rydberg electron is significantly perturbed by the confining potential especially for the values of $\omega$ close to the critical value $\omega_c$ (see Section 4.3).

It is interesting to observe that the studied Rydberg states respond differently to the applied confinement. For example, the equilibrium internuclear distance decreases for the $A\ ^2\Sigma^+$ state (similarly to the effect observed in strongly bound molecules such as $H_2$) while it increases for the $C\ ^2\Sigma^+$ state. In order to rationalize these differences in terms of the changes in the electron density induced by the confinement, additional calculations were performed for the $^2\Sigma^+$ states for the two values $\omega = 0.0$ and $\omega = 0.025$ au at the corresponding equilibrium internuclear distances (see table 3). As shown in figure 6 the confining potential of strength $\omega = 0.025$ au increases the density between the nuclei (and leads to the bond shortening) for the $A\ ^2\Sigma^+$ and $F\ ^2\Sigma^+$ states while in the $C\ ^2\Sigma^+$ and $D\ ^2\Sigma^+$ states the electron density, compressed under the influence of confinement, is depleted from the internuclear region, leading to bond lengthening.

The confining potential, by inducing spatial restrictions on the electron distribution, will lead to an increase in the electron correlation energy, defined as the difference between the Hartree-Fock energy and the full CI energy. Due to the lack of orthogonality between the Hartree-Fock solutions for the $\Sigma$ states, the calculations were done only for the lowest $\Pi$ state. The regular increase of the correlation energy for the $B\ ^2\Pi$ state is shown in figure 7 as the difference between the value for the confined and the unconfined system.

### *4.2. Transition dipole moments and oscillator strengths*

It has been shown by the molecular orbital analysis that the application of a confining potential alters the configurations of both the A and C states by introducing an avoided crossing between 2.5 to 3.0 au. This configuration interaction leads to the changes of the equilibrium internuclear distance $r_e$ and the binding energy of these states. In addition, this configuration mixing influences the intensities of the electronic transitions involving the A and C states. In order to examine the variation of the transition intensities with respect to $\omega$, the transition dipole moments for the transitions between the X, A, B,

and C states and the associated oscillator strengths (or $f$-values) were calculated.

The electronic transition dipole moment for an $N$-electron system can be defined in two ways [45]: in the dipole-length approximation

$$\langle\psi_f|\vec{\mu}|\psi_i\rangle = \int_\tau \psi_f^*(\mathbf{r}) \left( e \sum_{k=1}^{N} \mathbf{r}_k \right) \psi_i(\mathbf{r}) d\tau, \tag{6}$$

and in the dipole-velocity approximation

$$\langle\psi_f|\vec{\mu}|\psi_i\rangle = \frac{h}{4\pi^2 m_e \omega_{if}} \int_\tau \psi_f^*(\mathbf{r}) \sum_{k=1}^{N} \nabla_k \psi_i(\mathbf{r}) d\tau. \tag{7}$$

In these expressions $\psi_i$ and $\psi_f$ represent, respectively, the initial and final states of the transition and $\omega_{if}$ is the frequency of the radiation. The dimensionless oscillator strengths can be calculated from the following equation:

$$f_{i\to f} = \frac{8\pi^2 m_e}{3he^2} \omega_{if} |\langle\psi_f|\vec{\mu}|\psi_i\rangle|^2. \tag{8}$$

This quantity constitutes the measure of the probability of an electronic transition. Hence, the comparison of the $f$-values of different transitions can provide information regarding their intensity ratio, population densities, and lifetimes.

The equations 6 and 7 will yield different values of dipole transition moments if an approximate wavefunction is used [46]. Therefore, a test has been performed using both equations with the full CI wavefunction computed in the present study. It was found that the dipole transition moments (and, in turn, the oscillator strength) calculated by using both formulas differ by only 1 to 2 % for $^2\Sigma^+$ states. However, a larger difference of about 10 % was found for $^2\Pi$ states which is possibly due to the deficiency in the basis sets describing the $\pi$-electron density.

In spite of the less satisfactory agreement for the $^2\Pi$ states, the data from both calculations support the conclusion that the A and C states undergo an interchange of configurations when the HeH molecule is confined. In the case of $\omega = 0.0$ au the A $\rightarrow$ B transition moment is larger than the B $\rightarrow$ C transition moment for the studied range of $R$ (see figure 8). The B state has a dominant contribution from the hydrogen's $2p$ orbital. Therefore, it is expected that the A state, which is dominated by the $2s$ orbital of hydrogen, should lead to a large dipole transition moment. The B $\rightarrow$ C dipole transition moment increases at large $R$. This results from the enhanced $2s$ character of the C state, which has a dominant $2p$ configuration at intermediate $R$, when approaching the asymptotic limit where the $2s$ and $2p$ orbitals become degenerate.

The A $\rightarrow$ B dipole transition moment curve drops very rapidly under confinement which suggests that the A state loses a significant amount of $2s$ character due to the confinement. A crossing exists between the A $\rightarrow$ B and B $\rightarrow$ C transition moment curves and it shifts to smaller $R$ with increasing $\omega$. These changes indicate an important interaction between the A and C states due to which the C state attains the hydrogen $2s$ character. Interestingly, the increased $2s$ character of the C state does not affect very much the B $\rightarrow$ C dipole transition moment at large $R$ although its magnitude becomes larger than the A $\rightarrow$ B transition moment.

Because of the configuration mixing of the A and C states a prominent change in the peak intensities of the electronic spectrum is anticipated. Figure 9(a) shows the calculated oscillator strengths for both the A $\rightarrow$ B and B $\rightarrow$ C transitions. Clearly, the oscillator strength, and thus the transition intensity, for the B $\rightarrow$ C transition significantly increases with increasing $\omega$ at large $R$ which may be attributed to the increasing $2s$ character of the C state. On the other hand, the maximum for the A $\rightarrow$ B transition decreases which corresponds to the decreasing $2s$ character of the A state.

For comparison, the oscillator strengths for the X $\rightarrow$ A and X $\rightarrow$ C transitions were also computed and displayed in figure 9(b). Since the ground state of HeH is composed of the ground-state He($1s^2$) and H($1s$) the trend in the change of the transition probabilities, which are proportional to the oscillator strengths, for the X $\rightarrow$ A and X $\rightarrow$ C transitions should be opposite to that for the A $\rightarrow$ B and A $\rightarrow$ C transitions. As expected, the oscillator strength for the X $\rightarrow$ A transition increases at large $R$ for $\omega > 0.0$ since the increased $2p$ character of the A state brings about a stronger transition to the X state. Conversely, the $2s$ character of the C state reduces the transition probability of the X $\rightarrow$ C transition quite considerably. A surprising feature is noticed in the small $R$ region where the transition probability for the X $\rightarrow$ C transition sharply increases at $R = 1.0$ au. This observation indicates that in the small $R$ regime the $2p_z$ orbitals are more destabilized and lie at higher energy than the $2s$-orbital in contrast to the situation in the intermediate $R$ range where the $2p_z$ orbital is more stable than the $2s$ orbital in the presence of a cylindrical confining potential.

### *4.3. Critical confinement and ionization*

When an atom or molecule is excited into an energy level that lies above its first ionization limit the system will become unstable and a spontaneous ionization will occur in which an electron will be ejected. This process is referred to as auto-ionization or field-induced ionization [47]. As the valence electrons of the Rydberg molecules are only weakly bound to the parent ion core it is expected that they could be expelled easily by an external potential.

In order to determine the strength of confinement at which an electronic state of HeH undergoes auto-ionization, the following quantity

$$\Delta E^n(\omega) = E^n_{\mathrm{HeH}}(\omega; r_e) - E^0_{\mathrm{HeH}^+}(\omega; r_e), \tag{9}$$

was computed where $n = 1, 2, \ldots$ is the index of the excited state, i.e. A ($n = 1$), B ($n = 2$) and so on, while $n = 0$ refers to the ground state and $r_e$ is the equilibrium internuclear distance of the HeH molecule. The critical confinement is defined by the value of $\omega$ at which $\Delta E^n = 0$. The results obtained using the method described in the earlier study of NeH [43] are plotted in figure 10 and summarized in table 4. As might be expected the higher the excitation, i.e. the larger $n$, the smaller the confinement parameter $\omega_c$ due to the more diffuse spatial distribution of the Rydberg electron density. It is interesting to note that the values of $\omega_c$ obtained in the present study for HeH are larger than the corresponding values for the analogous NeH molecule [43]. This

observation reveals that the Rydberg electron in HeH is indeed more strongly bound by the $HeH^+$ core than the Rydberg electron in the NeH molecule. This is consistent with the earlier finding that the H($2p$) Rydberg orbital of HeH, estimated by the location of the potential barrier of the C state potential, is slightly smaller than that of NeH. These two phenomena can be accounted for by the weaker attraction between the $NeH^+$ core and the Rydberg electron due to the screening effect of the Ne electron cloud. The less-effective shielding in HeH results in a stronger binding of the Rydberg electron and a smaller Rydberg orbital.

## 5. Final remarks

The Rydberg molecule HeH confined by a cylindrical harmonic potential has been investigated and it has been found that confinement affects this molecule differently than strongly-bound diatomic molecules. The effects of the confining potential on the molecular properties of HeH have been studied. The confinement does not dramatically vary the bond lengths for the low-lying electronic states of HeH and the bond lengths could be either stretched or compressed. The excited states are not necessarily more strongly bound by the potential. It has been found that some of the states become even less bound when a confining potential is applied. While the lowest states in each symmetry, $X\ ^2\Sigma^+$ and $B\ ^2\Pi$, retain their configurations for the whole range of $R$ there appears a new avoided crossing between the A and C states where they interchange the dominant configurations. This configuration mixing is manifested in the variation of the dipole transition moments and the oscillator strengths of the electronic transitions involving these states.

It is predicted that this system will be easily ionized by even a modestly strong confining potential. For the higher excited states weaker potentials are required to trigger the process of auto-ionization.

## Acknowledgments

This work was financially supported by the Natural Science and Engineering Research Council of Canada (NSERC) (PGS-B Scholarship to JMHL and NSERC Research Grant to MK). DBW thanks the Polish Ministry of Science and Information Society Technologies, Grant No. 2PO3B 033 25. Helpful comments by Dr. J. Karwowski and insightful remarks of an anonymous Referee are highly appreciated.

## References

[1] Mukherjee P K, Karwowski J and Diercksen G H F 2002 *Chem. Phys. Lett.* **363** 323
[2] Bielińska-Wąż D, Karwowski J, Saha B and Mukherjee P K 2003 *Phys. Rev.* E **68** 016404 1-6
[3] Kappes U and Schmelcher P 1995 *Phys. Rev.* A **51** 4542
[4] Rosei F and Rosei R 2002 *Surf. Science* **500** 395

[5] Rosei F, Schunack M, Jiang P, Gourdon A, Lægsgaard E, Stensgaard I, Joachim C and Besenbacher F 2002 *Science* **296** 328
[6] Jaskólski W 1996 *Phys. Rep.* **271** 1
[7] Connerade J-P, Dolmatov V K, Lakshmi P A 2000 *J. Phys. B: At. Mol. Opt. Phys.* **33** 251
[8] Connerade J-P and Kengkan P 2003 *Proc. Idea-Finding Symposium, Frankfurt Institute for Advanced Studies* (Debrecen: EP Systema) pp. 35-46
[9] Bielińska-Wąż D, Karwowski J and Diercksen G H F 2001 *J. Phys. B: At. Mol. Opt. Phys.* **34** 1987
[10] Sako T and Diercksen G H F 2003 *J. Phys. B: At. Mol. Opt. Phys.* **36** 1433
[11] Sako T and Diercksen G H F 2003 *J. Phys. B: At. Mol. Opt. Phys.* **36** 1681
[12] Bielińska-Wąż D, Diercksen G H F and Klobukowski M 2001 *Chem. Phys. Lett.* **349** 215
[13] Lai D, Salpeter E E and Shapiro S L 1992 *Phys. Rev.* A **45** 4832
[14] Sako T, Černušák I and Diercksen G H F, 2004 *J. Phys. B: At. Mol. Opt. Phys.* **37** 1091
[15] Lo J M H, Klobukowski M and Diercksen G H F 2005 *Adv. Quantum Chem.* **48** 59
[16] Michels H H and Harris F E 1963 *J. Chem. Phys.* **39** 1464
[17] Theodorakopoulos G, Farantos S C, Buenker R J and Peyerimhoff S D, 1984 *J. Phys. B: At. Mol. Phys.* **17** 1453
[18] Möller T, Beland M and Zimmerer G 1985 *Phys. Rev. Lett.* **55** 2145
[19] Möller T, Beland M and Zimmerer G 1987 *Chem. Phys. Lett.* **136** 551
[20] Kubach C, Sidis V, Fussen D and van der Zande J 1987 *Chem. Phys.* **117** 439
[21] Ketterle W 1989 *Phys. Rev. Lett.* **62** 1480
[22] Tokaryk D W, Brooks R L and Hunt J L 1989 *Phys. Rev.* A **40** 6113
[23] Ketterle W, Dodhy A and Walther H 1988 *J. Chem. Phys.* **89** 3442
[24] Ketterle W 1990 *J. Chem. Phys.* **93** 3752
[25] Ketterle W 1990 *J. Chem. Phys.* **93** 3760
[26] Ketterle W 1990 *J. Chem. Phys.* **93** 6929
[27] Ketterle W, Messmer H P and Walther H 1989 *Phys. Rev.* A **40** 7434
[28] Sarpal B K, Branchett S E, Tennyson J and Morgan L A 1991 *J. Phys. B: At. Mol. Opt. Phys.* **24** 3685
[29] Rhodes C K 1984 *Topics in Applied Physics. Excimer Lasers* 2nd ed (Berlin: Springer)
[30] Herzberg G 1987 *Annu. Rev. Phys. Chem.* **38** 27
[31] Sommerfeld A and Welker H 1938 *Annalen Phys., Lpz.* **32** 56
[32] Diercksen G H F and Hall G G 1994 *Comput. Phys.* **8** 215
[33] Schmidt M W, Baldridge K K, Boatz J A, Elbert S T, Gordon M S, Jensen J J, Koseki S, Matsunaga N, Nguyen K A, Su S, Windus T L, Dupuis M and Montgomery J A 1993 *J. Comp. Chem.* **14** 1347
[34] Ivanic J and Ruedenberg K 2001 *Theoret. Chem. Acc.* **106** 339
[35] Römelt J, Peyerimhoff S D and Buenker R J 1978 *Chem. Phys.* **34** 403
[36] Schreiner E W S 1996 *Ph.D. Thesis* (München: Technische Universität)
[37] Huzinaga S 1965 *J. Chem. Phys.* **42** 1293
[38] Theodorakopoulos G, Petsalakis I D, Nicolaides C A and Buenker R J 1987 *J. Phys. B: At. Mol. Phys.* **20** 2339
[39] Ketterle W, Figger H and Walther H 1985 *Phys. Rev. Lett.* **55** 2941
[40] Wolniewicz L 1965 *J. Chem. Phys.* **43** 1087
[41] Kolos W and Peek J M 1976 *Chem. Phys.* **12** 381
[42] Petsalakis I D, Theodorakopoulos G, Nicolaides C A and Buenker R J 1987 *J. Phys. B: At. Mol. Opt. Phys.* **20** 5959
[43] Lo J M H, Klobukowski M, Bielińska-Wąż D, Diercksen G H F and Schreiner E W S, 2005 *J. Phys. B: At. Mol. Opt. Phys.* **38** 1143
[44] Detmer T, Schmelcher P, Diakonos F K and Cederbaum L S 1997 *Phys. Rev.* A **56** 1825
[45] Bates D R 1951 *J. Chem. Phys.* **19** 1122

[46] Chandrasekhar S 1945 *Astrophys. J. 102* 223
[47] Thorne A, Litzén U and Johansson S 1999 *Spectrophysics: Principles and Applications* (New York: Springer)

## Tables and table captions

**Table 1.** Spectroscopic constants of HeH without confinement ($r_e$ in atomic units, $\nu_e$ and $\nu_e x_e$ in $\mathrm{cm}^{-1}$, $D_e$ in eV)

| State | Reference | $r_e$ | $\nu_e$ | $\nu_e x_e$ | $D_e$ |
|---|---|---|---|---|---|
| A $^2\Sigma^+$ | He-21/H-18 | 1.4077 | 3670 | 255 | 2.53 |
| | He-21/H-36 | 1.4118 | 3699 | 196 | 2.54 |
| | He-21/H-55 | 1.4149 | 3722 | 183 | 2.54 |
| | He-34/H-55 | 1.4120 | 3726 | 182 | 2.54 |
| | [28] | 1.4040 | 3512 | | |
| | [38] | 1.4115 | 3662 | | 2.48 |
| | [39] | 1.43 | 3701 | | |
| | [23] | 1.4003 | 3718 | 161 | |
| B $^2\Pi$ | He-21/H-18 | 1.4634 | 3364 | 199 | 2.21 |
| | He-21/H-36 | 1.4629 | 3330 | 205 | 2.18 |
| | He-21/H-55 | 1.4652 | 3367 | 201 | 2.19 |
| | He-34/H-55 | 1.4622 | 3372 | 199 | 2.20 |
| | [28] | 1.4571 | 3158 | | |
| | [38] | 1.4629 | 3302 | | 2.20 |
| C $^2\Sigma^+$ | He-21/H-18 | 1.5413 | 2928 | 210 | 1.64 |
| | He-21/H-36 | 1.5409 | 2930 | 190 | 1.61 |
| | He-21/H-55 | 1.5417 | 3007 | 199 | 1.61 |
| | He-34/H-55 | 1.5370 | 2957 | 211 | 1.61 |
| | [28] | 1.5255 | 2788 | | |
| | [38] | 1.5428 | 2872 | | 1.65 |
| | [39] | 1.57 | 2896 | | |
| | [23] | 1.5324 | 2902 | 141 | |
| D $^2\Sigma^+$ | He-21/H-18 | 1.4545 | 3418 | 196 | 2.18 |
| | He-21/H-36 | 1.4479 | 3467 | 289 | 2.16 |
| | He-21/H-55 | 1.4584 | 3402 | 202 | 2.15 |
| | He-34/H-55 | 1.4555 | 3405 | 201 | 2.16 |
| | [28] | 1.4504 | 3187 | | |
| | [38] | 1.4508 | 3383 | | 2.14 |
| E $^2\Pi$ | He-21/H-18 | 1.4719 | 3296 | 204 | 2.09 |
| | He-21/H-36 | 1.4725 | 3258 | 193 | 2.08 |
| | He-21/H-55 | 1.4736 | 3297 | 207 | 2.07 |
| | He-34/H-55 | 1.4708 | 3299 | 207 | 2.08 |
| | [28] | 1.4655 | 3083 | | |
| | [38] | 1.4718 | 3233 | | 2.09 |
| F $^2\Sigma^+$ | He-21/H-18 | 1.5518 | 3013 | 209 | 1.46 |
| | He-21/H-36 | 1.4696 | 3276 | 303 | 2.03 |
| | He-21/H-55 | 1.4801 | 3246 | 209 | 2.05 |
| | He-34/H-55 | 1.4771 | 3252 | 208 | 2.06 |
| | [28] | 1.4693 | 3057 | | |

**Table 2.** Spectroscopic constants of $HeH^+$ in the $^1\Sigma^+$ state without confinement ($r_e$ in atomic units, $\nu_e$ and $\nu_e x_e$ in $cm^{-1}$)

| Reference | $r_e$ | $\nu_e$ | $\nu_e x_e$ |
|---|---|---|---|
| He-21/H-36 | 1.4770 | 3177 | 141 |
| He-21/H-36 | 1.4694 | 3275 | 149 |
| He-21/H-55 | 1.4765 | 3201 | 145 |
| He-34/H-55 | 1.4732 | 3206 | 146 |
| [16] | 1.444 | 3379 | 314 |
| [40] | 1.4632 | $3233^{(a)}$ | $617^{(a)}$ |
| [41] | 1.4632 | $3220^{(a)}$ | $166^{(a)}$ |

(a) Calculated by fitting Wolniewicz and Kolos' *ab initio* potential energy curves to Dunham's 4-th order polynomial.

**Table 3.** Equilibrium internuclear distance $r_e$ (in atomic units) for different electronic states of HeH

| $\omega$ | State | | | | | |
|---|---|---|---|---|---|---|
| (au) | A $^2\Sigma^+$ | B $^2\Pi$ | C $^2\Sigma^+$ | D $^2\Sigma^+$ | E $^2\Pi$ | F $^2\Sigma^+$ |
| 0.000 | 1.4118 | 1.4629 | 1.5409 | 1.4573 | 1.4725 | 1.4800 |
| 0.025 | 1.4055 | 1.4622 | 1.5571 | 1.4686 | 1.4788 | 1.4546 |
| 0.050 | 1.3922 | 1.4594 | 1.5824 | 1.4661 | 1.4803 | 1.4478 |
| 0.075 | 1.3783 | 1.4558 | 1.6165 | | | |
| 0.100 | 1.3660 | 1.4491 | 1.6521 | | | |
| 0.125 | 1.3542 | 1.4435 | | | | |
| 0.150 | 1.3430 | | | | | |

**Table 4.** Critical confinement $\omega_c$ for different electronic states of HeH

| State | $\omega_c$ (au) |
|---|---|
| A $^2\Sigma^+$ | 0.178 |
| B $^2\Pi$ | 0.155 |
| C $^2\Sigma^+$ | 0.111 |
| D $^2\Sigma^+$ | 0.067 |
| E $^2\Pi$ | 0.055 |
| F $^2\Sigma^+$ | 0.042 |

**Figure captions**

Figure 1: Potential energy curves of selected low-lying electronic states of HeH and of the ground state of $HeH^+$. The solid and dotted lines are the potential energy curves of the $^2\Sigma^+$ states of HeH and the dashed line is the X $^1\Sigma^+$ state of $HeH^+$.

Figure 2: Potential energy curves of the low-lying excited states A $^2\Sigma^+$ (a), B $^2\Pi$ (b), C $^2\Sigma^+$ (c) of HeH and of the X $^1\Sigma^+$ (d) ground state of $HeH^+$ in confinement. The bottom line corresponds to $\omega = 0.0$ au and the successive lines correspond to increments in $\omega$ of 0.025 au.

Figure 3: Potential energy curves of the excited states A $^2\Sigma^+$ (solid line) and C $^2\Sigma^+$ (dashed line) of HeH in the field-free case (a) and in confinement with strength $\omega$ of 0.05 au (b) , 0.075 au (c) , and 0.10 au (d).

Figure 4: Variation of the equilibrium internuclear distances $r_e$ with the strength of the confinement. The distances are shown for the states A $^2\Sigma^+$ (+), B $^2\Pi^+$ (■), C $^2\Sigma^+$ (×), D $^2\Sigma^+$ ( △), E $^2\Pi^+$ (○ ), and F $^2\Sigma^+$ (□).

Figure 5: Variation of the electric dipole moment $\mu$ for $R = 1.5$ au with the strength of the confinement. The results are shown for the states A $^2\Sigma^+$ (+), B $^2\Pi^+$ (■), C $^2\Sigma^+$ (×), D $^2\Sigma^+$ ( △), E $^2\Pi^+$ (○ ), and F $^2\Sigma^+$ (□).

Figure 6: Electron density difference for the A $^2\Sigma^+$ (a), C $^2\Sigma^+$ (b), D $^2\Sigma^+$ (c), and F $^2\Sigma^+$ (d) states. The solid contours indicate regions of increased electron density and the dashed contours the regions of reduced electron density induced by the confinement with strength $\omega = 0.025$ au. The outermost solid contours (marked with 1) correspond to 0.0003 au and the consecutive contours correspond to an increase in steps of 0.0003 au. The outermost dashed contours (marked with 2) correspond to -0.0003 au and the consecutive contours correspond to a decrease in steps of -0.0003 au.

Figure 7: Change in the electron correlation energy for the $B$ $^2\Pi$ state. The bottom line displays $E_{\rm corr}(\omega = 0.025) - E_{\rm corr}(\omega = 0.0)$; the lines above it are for the steps of 0.025 au in $\omega$.

Figure 8: Transition dipole moments as functions of the internuclear distance $R$. Solid-lines correspond to A-B transitions and dashed-lines correspond to B-C transitions.

Figure 9: Change of oscillator strengths with internuclear distance $R$. (a) Transitions between excited states. Solid lines correspond to A-B transitions and dashed lines correspond to B-C transitions. (b) Transitions from the ground state. Solid lines correspond to X-A transitions and dashed lines correspond to X-C transitions.

Figure 10: $\Delta E^n(\omega)$ (equation 9) for the studied electronic states of HeH as function of the confinement strength. The lines correspond to the following values of $n$ (states): $n = 1$ (A $^2\Sigma^+$) ——; $n = 2$ (B $^2\Pi^+$) — · —; $n = 3$ (C $^2\Sigma^+$) — — —; $n = 4$ (D $^2\Sigma^+$) - - - -; $n = 5$ (E $^2\Pi^+$) — · —; $n = 6$ (F $^2\Sigma^+$) · · · · · ·

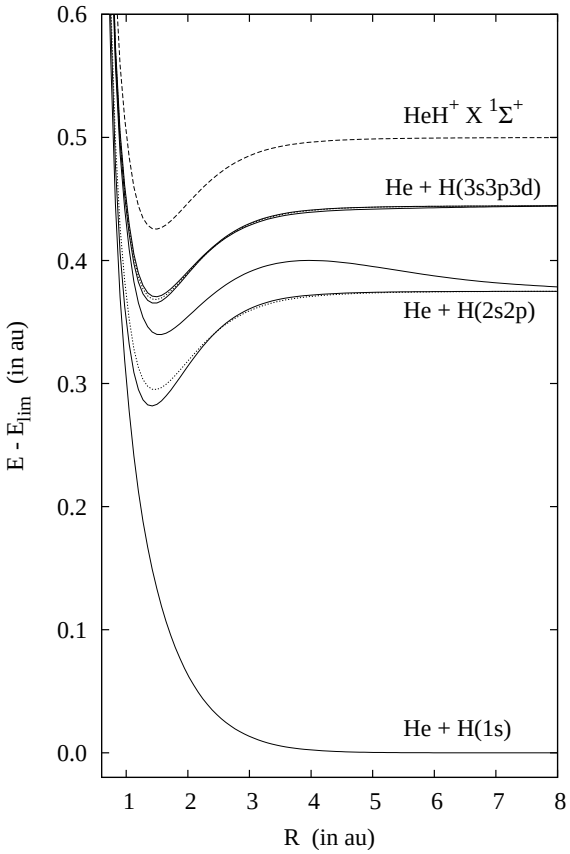


**Figure 1.** Potential energy curves of selected low-lying electronic states of HeH and of the ground state of $HeH^+$. The solid and dotted lines are the potential energy curves of the $^2\Sigma^+$ states of HeH and the dashed line is the X $^1\Sigma^+$ state of $HeH^+$.

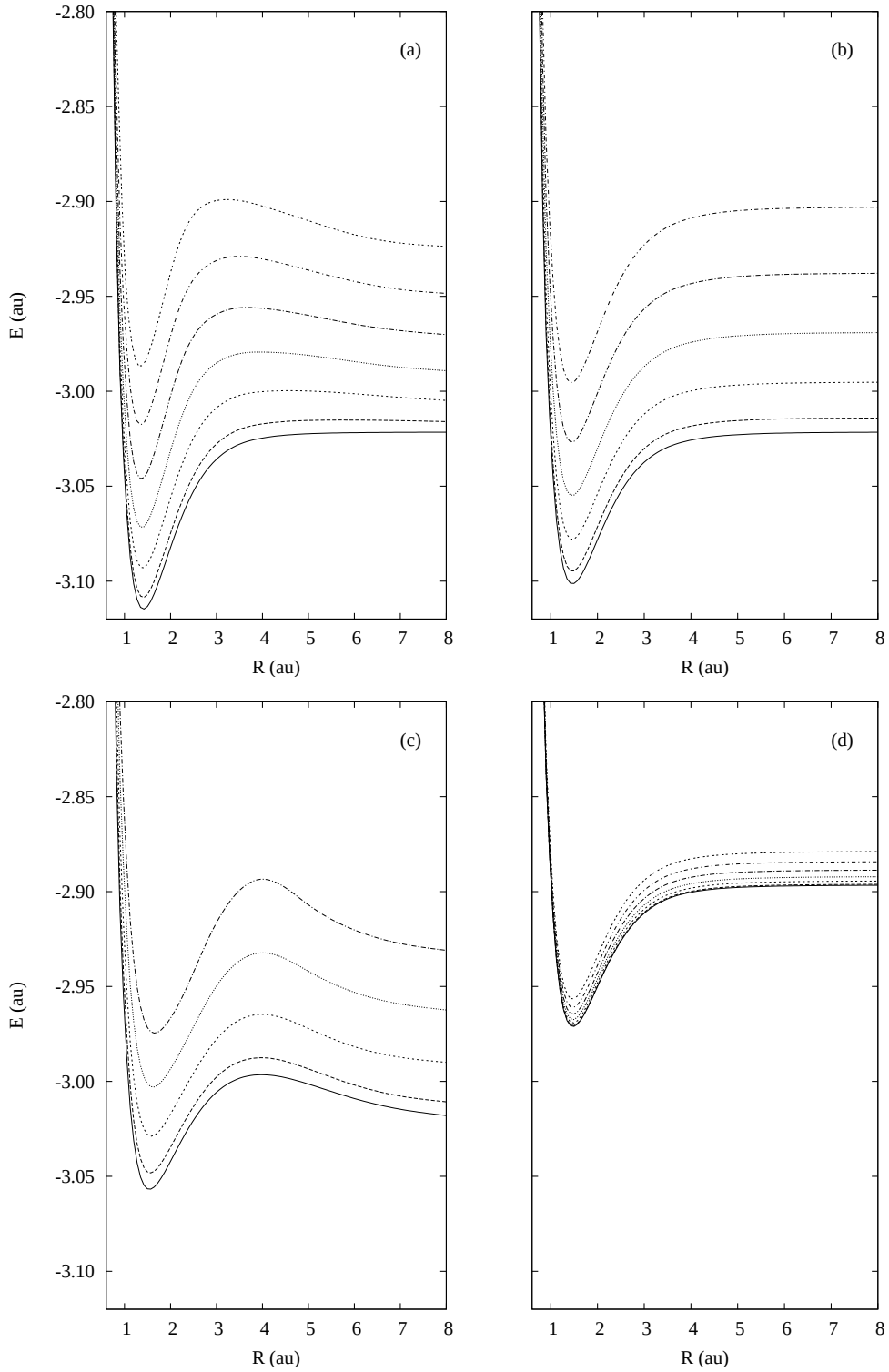


**Figure 2.** Potential energy curves of the low-lying excited states A $^2\Sigma^+$ (a), B $^2\Pi$ (b), C $^2\Sigma^+$ (c) of HeH and of the X $^1\Sigma^+$ (d) ground state of $HeH^+$ in confinement. The bottom line corresponds to $\omega = 0.0$ au and the successive lines correspond to increments in $\omega$ of 0.025 au.

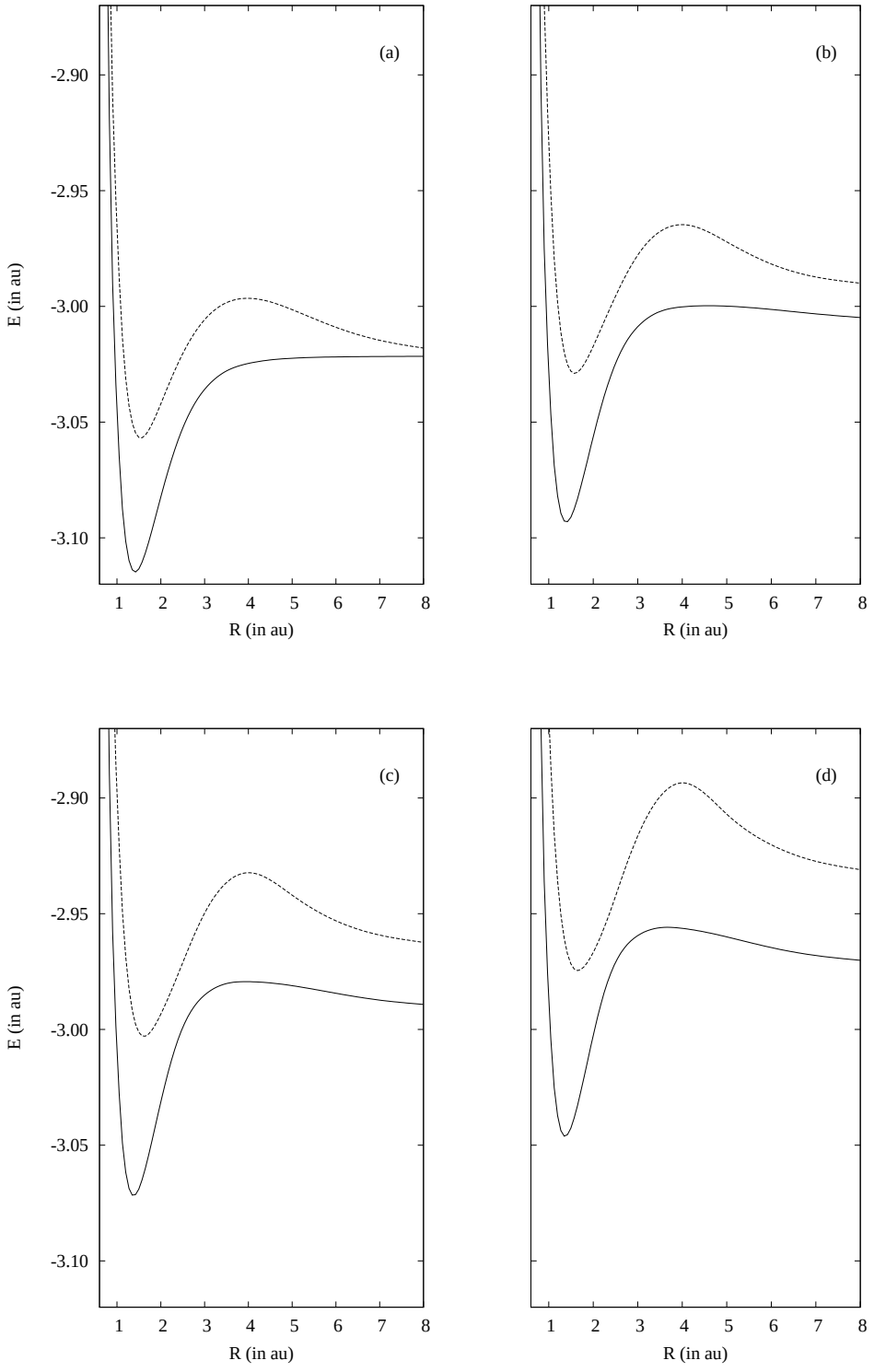


**Figure 3.** Potential energy curves of the excited states A $^2\Sigma^+$ (solid line) and C $^2\Sigma^+$ (dashed line) of HeH in the field-free case (a) and in confinement with strength $\omega$ of 0.05 au (b), 0.075 au (c), and 0.10 au (d).

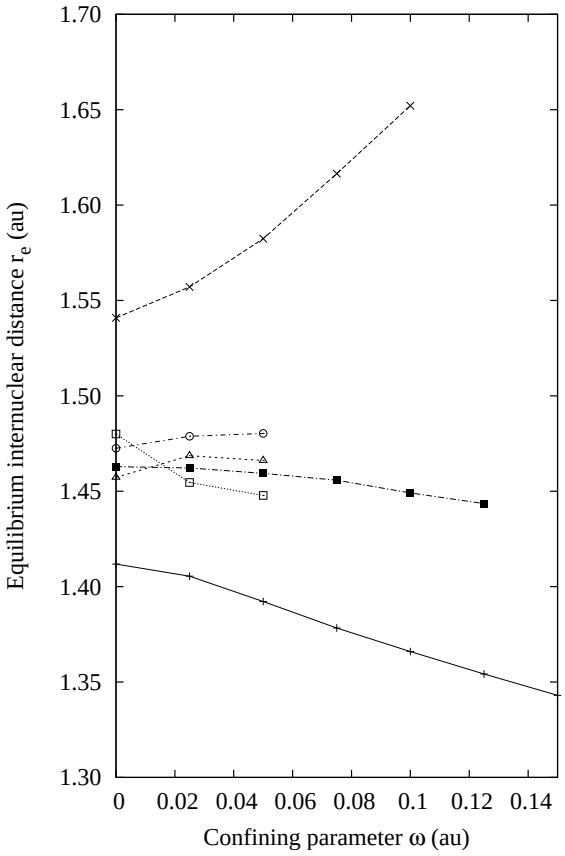


**Figure 4.** Variation of the equilibrium internuclear distances $r_e$ with the strength of the confinement. The distances are shown for the states A $^2\Sigma^+$ (+), B $^2\Pi^+$ (■), C $^2\Sigma^+$ (×), D $^2\Sigma^+$ ( △), E $^2\Pi^+$ (○ ), and F $^2\Sigma^+$ (□).

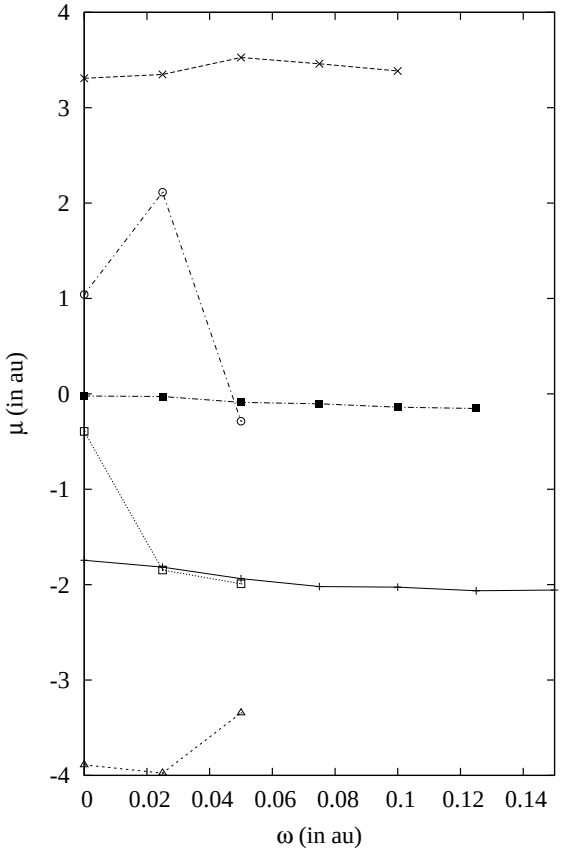


**Figure 5.** Variation of the electric dipole moment $\mu$ for $R = 1.5$ au with the strength of the confinement. The results are shown for the states A $^2\Sigma^+$ (+), B $^2\Pi^+$ (■), C $^2\Sigma^+$ (×), D $^2\Sigma^+$ ( △), E $^2\Pi^+$ (○ ), and F $^2\Sigma^+$ (□).

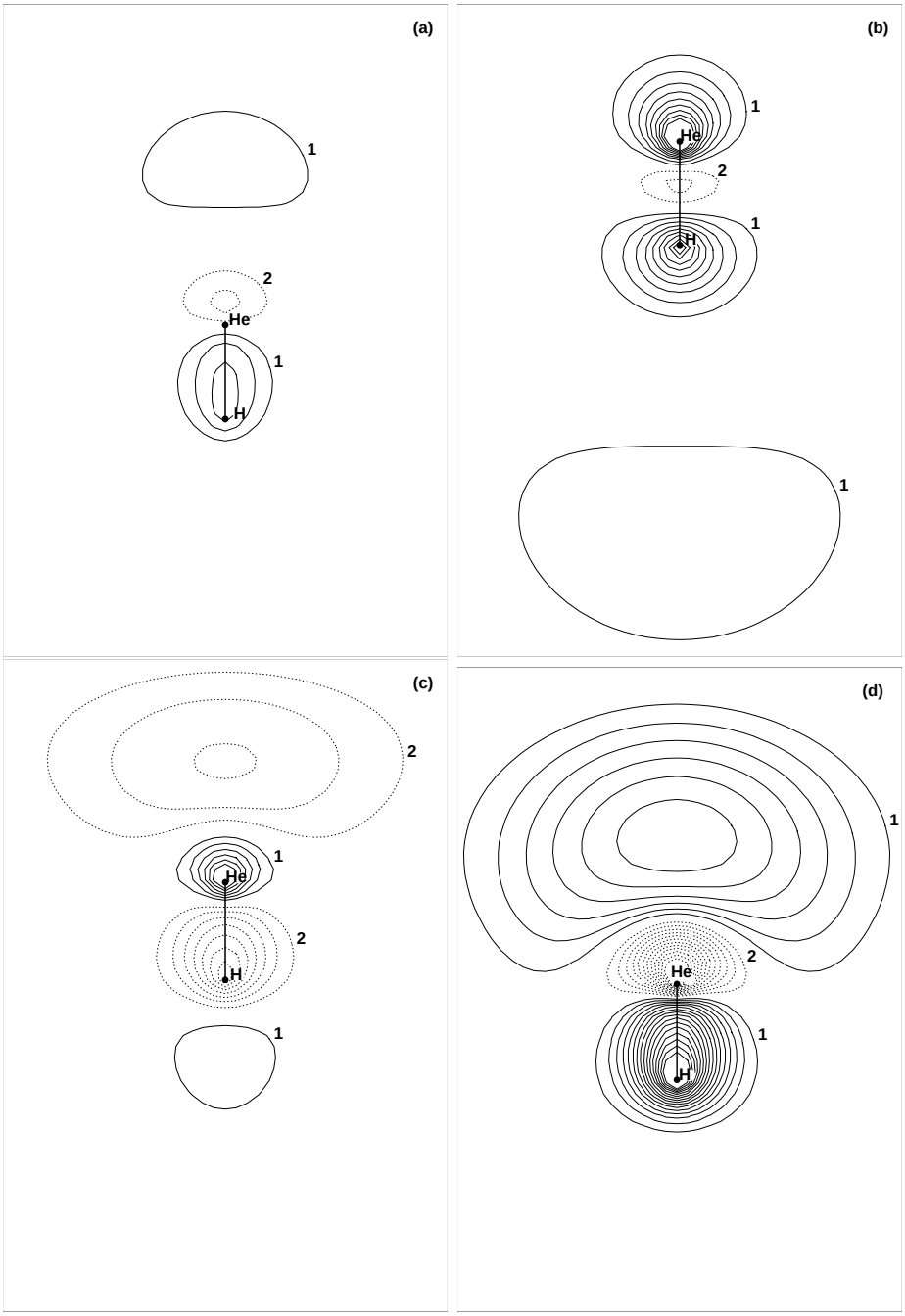


**Figure 6.** Electron density difference for the A $^2\Sigma^+$ (a), C $^2\Sigma^+$ (b), D $^2\Sigma^+$ (c), and F $^2\Sigma^+$ (d) states. The solid contours indicate regions of increased electron density and the dashed contours the regions of reduced electron density induced by the confinement with strength $\omega = 0.025$ au. The outermost solid contours (marked with 1) correspond to 0.0003 au and the consecutive contours correspond to an increase in steps of 0.0003 au. The outermost dashed contours (marked with 2) correspond to -0.0003 au and the consecutive contours correspond to a decrease in steps of -0.0003 au.

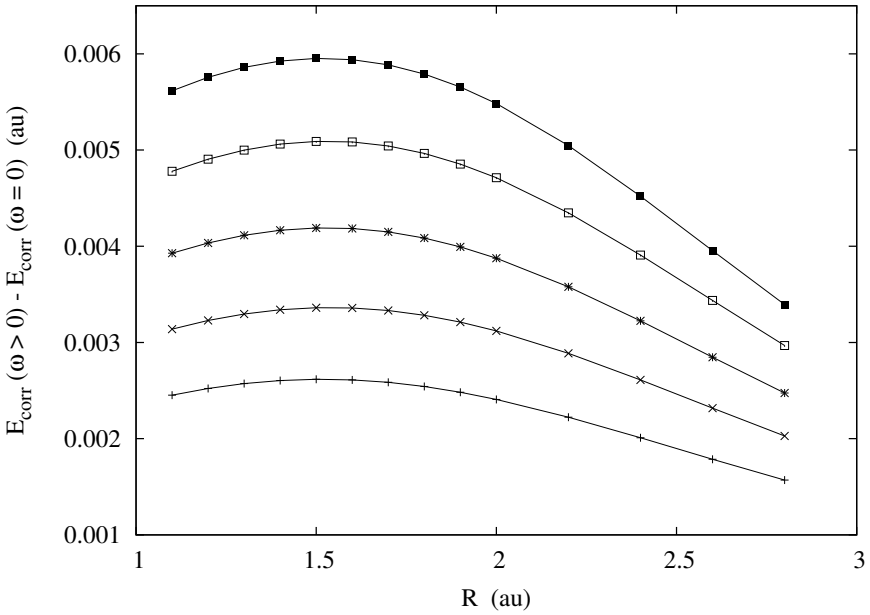


**Figure 7.** Change in the electron correlation energy for the $B\ ^2\Pi$ state. The bottom line displays $E_{\rm corr}(\omega = 0.025) - E_{\rm corr}(\omega = 0.0)$; the lines above it are for the steps of 0.025 au in $\omega$.

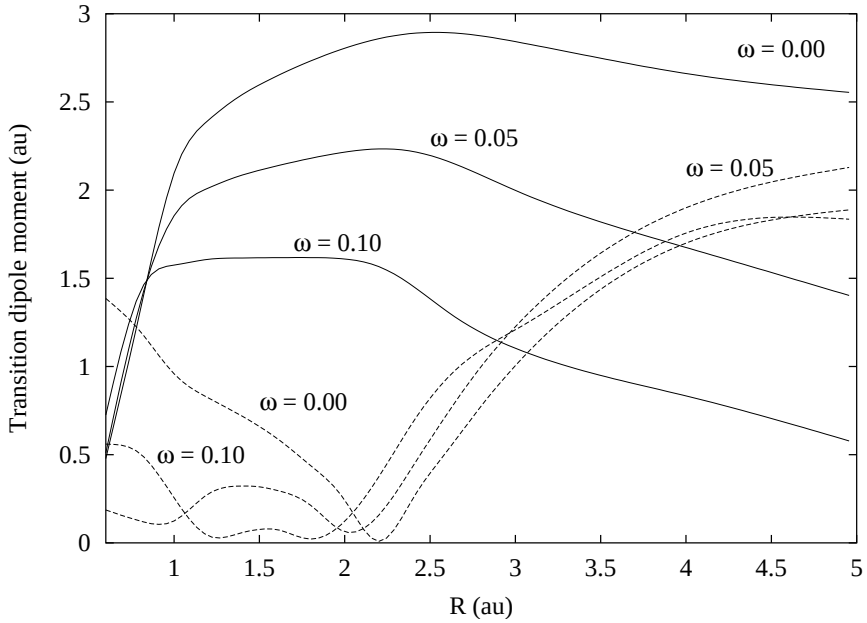


**Figure 8.** Transition dipole moments as functions of the internuclear distance $R$. Solid-lines correspond to A-B transitions and dashed-lines correspond to B-C transitions.

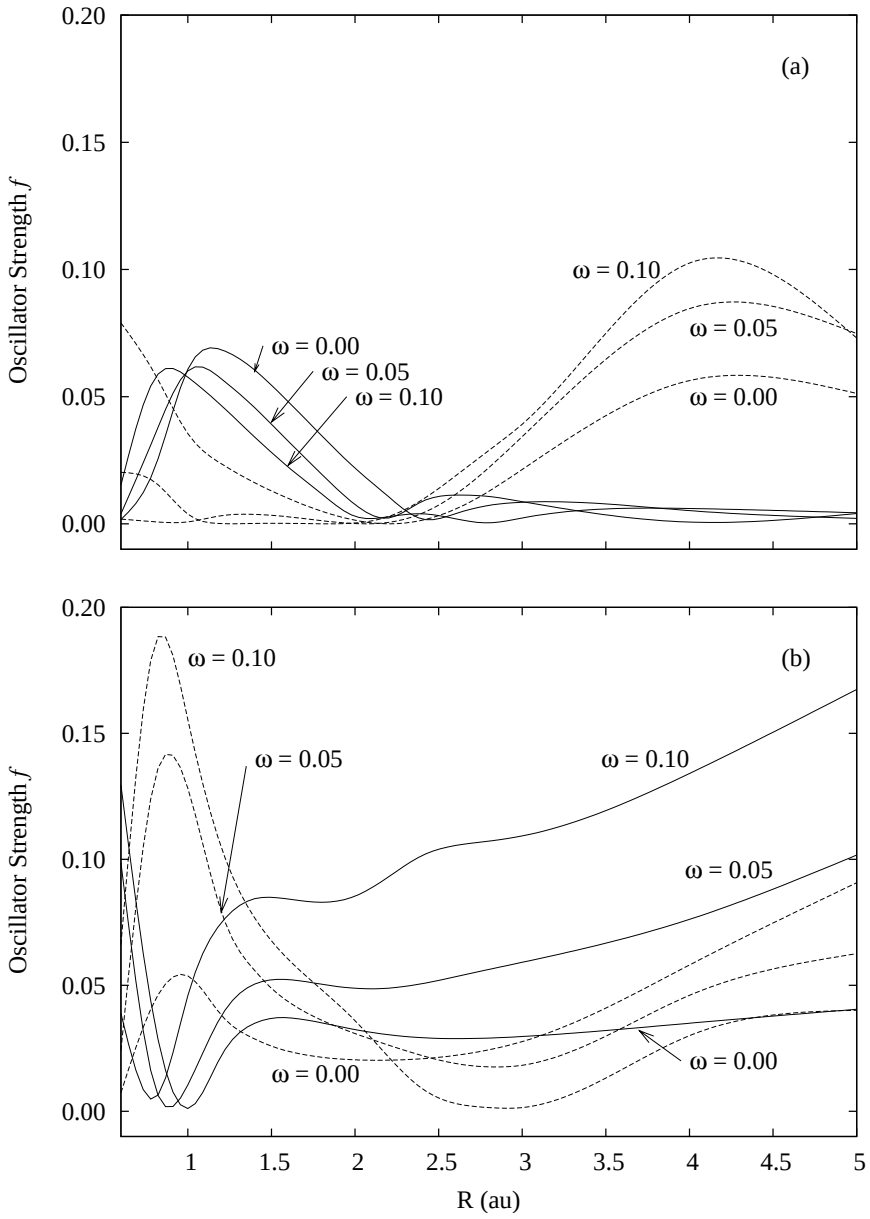


**Figure 9.** Change of oscillator strengths with internuclear distance $R$. (a) Transitions between excited states. Solid lines correspond to A-B transitions and dashed lines correspond to B-C transitions. (b) Transitions from the ground state. Solid lines correspond to X-A transitions and dashed lines correspond to X-C transitions.

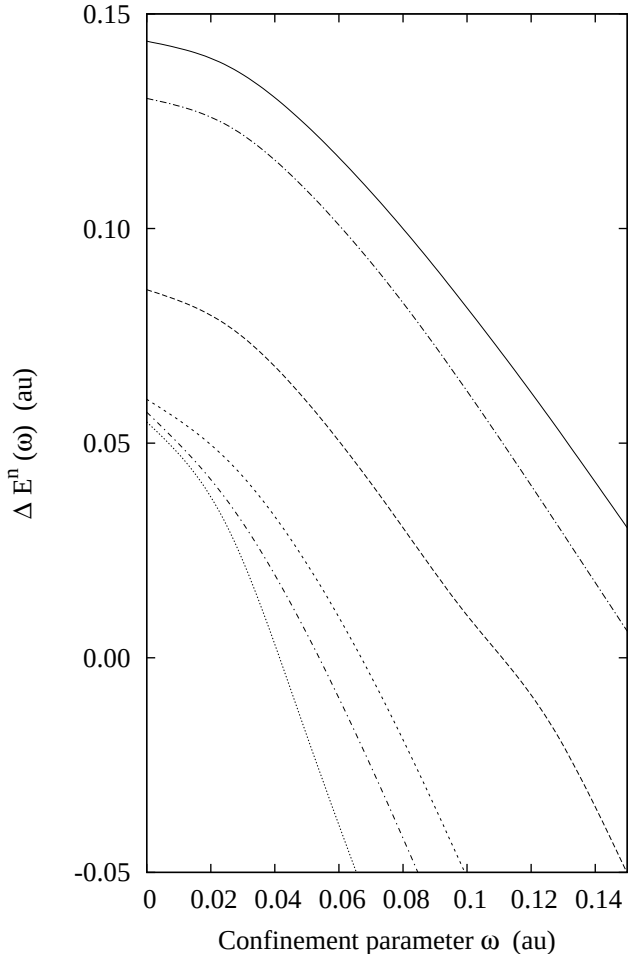


**Figure 10.** $\Delta E^n(\omega)$ (equation 9) for the studied electronic states of HeH as function of the confinement strength. The lines correspond to the following values of $n$ (states): $n = 1$ ($\mathrm{A}\,^2\Sigma^+$) ——; $n = 2$ ($\mathrm{B}\,^2\Pi^+$) — · —; $n = 3$ ($\mathrm{C}\,^2\Sigma^+$) — — —; $n = 4$ ($\mathrm{D}\,^2\Sigma^+$) - - - -; $n = 5$ ($\mathrm{E}\,^2\Pi^+$) — · —; $n = 6$ ($\mathrm{F}\,^2\Sigma^+$) · · · · · ·